ELSEVIER

Contents lists available at ScienceDirect

Marine Chemistry

journal homepage: www.elsevier.com/locate/marchem





Dynamics of chromophoric dissolved organic matter in a highly productive Amundsen Sea polynya

Ji Hu^a, Siyou Xue^{a,b}, Jun Zhao^a, Zhengbing Han^a, Dong Li^a, Haifeng Zhang^a, Peisong Yu^a, Minhui Zheng^a, Jianming Pan^{a,*}, Yongge Sun^c

- ^a Key Laboratory of Marine Ecosystem Dynamics, Second Institute of Oceanography, Ministry of Natural Resources, China
- ^b College of Ocean and Earth Sciences, Xiamen University, China
- ^c Organic Geochemistry Unit, School of Earth Sciences, Zhejiang University, China

ARTICLE INFO

Keywords: Chromophoric dissolved organic matter Microbial degradation Polynya, Amundsen Sea Antarctica

ABSTRACT

Dissolved organic carbon (DOC) is the largest organic carbon pool in the ocean, and is the most active component in respect to the ocean carbon cycling. However, its study in Antarctica has been limited due to challenges associated with sample collection. In this study, we conduct an investigation on the chromophoric dissolved organic matter (CDOM) in a highly productive Amundsen Sea Polynya (ASP), where phytoplankton blooms occur annually during the austral summer, serving as the primary source of DOC and CDOM. The relative abundances of CDOM, as indicated by the absorption coefficient at 254 nm (a_{254}), exhibit significant variability, reaching up to 6.34 m $^{-1}$. Four fluorescent components, including two humic-like components (C1 and C4) and two protein-like components (C2 and C3), are identified by excitation emission matrix coupled with parallel factor analysis (EEM-PARAFAC). Our findings suggest that heterotrophic metabolism primarily contributes to the formation of humic-like fluorescent components and DOC removal. Water mass, solar radiation, primary productivity as well as microbial degradation are identified as the main factors influencing CDOM dynamics in ASP. This study bears significant implications for advancing our understandings of the CDOM and DOC dynamics in the coastal polynyas of Antarctica, thus facilitating improved evaluation of carbon cycle in the Antarctica.

1. Introduction

The Southern Ocean plays a critical role in the global carbon cycling, and it accounts for over 40% of the global oceanic anthropogenic CO2 uptake (Sallee et al., 2012). The polynyas surrounding Antarctica exhibited high productivity (Arrigo and van Dijken, 2003), and thus have long been recognized as a strong sink zone for CO₂ (Arrigo et al., 2008). The Amundsen Sea is located between Ross Sea and the BelingsGaujin Sea of the west Antarctica, which is one of the most affected regions by rapid global warming among the Antarctic marginal seas. Recent satellite images have revealed surface warming and reduced sea ice in this area, accompanied by the rapid melting and thinning of adjacent glacier (Schoof, 2010). The Amundsen Sea Polynya (ASP) has been identified as having the highest primary production among 37 identified coastal polynyas in the Southern Ocean. This is attributed to the infusion of iron from melting glaciers, which typically occurs in inshore area at austral summer (Arrigo and van Dijken, 2003). The increased productivity resulting from glacial retreat in the polynya

region could significantly impact the marine carbon cycle of Southern Ocean. Despite the dissolved organic matter (DOM) being the largest organic carbon reservoir in the ocean and playing a vital role in the ocean carbon cycling (Hansell and Carlson, 2013), our understanding of DOM dynamics in the ASP remains limited.

Chromophoric dissolved organic matter (CDOM) is the optically active component of DOM (Coble, 2007), which can absorb light at visible and ultraviolet wavelengths (Kieber et al., 1989). CDOM not only affects the optical properties of water column but also influences biogeochemical process, cycling of carbon, and trace elements (Nelson and Siegel, 2013). By modulating the light attenuation in the ocean, CDOM protects marine organisms from UV radiation, particularly in the Southern Ocean, where the highest levels of UV radiation occur at the end of December (Hansell, 2002; Norman et al., 2011; Osburn et al., 2009). Phytoplankton are generally considered the primary source of CDOM in open ocean due to the large amount of organic matter produced via photosynthesis (Carder et al., 1989). This coupling relationship has been observed by satellite images at a global scale (Siegel et al.,

^{*} Corresponding author.

E-mail address: jmpan@sio.org.cn (J. Pan).

2002) and regionally in-situ investigations (Babin et al., 2003). However, a decoupling relationship between CDOM and *Chl a* has also been found (Rochelle-Newall and Fisher, 2002), and bacteria contributions to CDOM have been reported both in the field and in the lab (Nelson et al., 1998; Ortega-Retuerta et al., 2009). Solar radiation can induce both photobleaching and photohumification processes in CDOM. Photobleaching causes the loss of absorbance due to the reaction of solar radiation (especially UV) with CDOM (Kieber et al., 1989), while photohumification can increase CDOM absorbance through the transformation of organic compounds such as fatty acids or triglycerides into humic-like substances (Kieber and Seaton, 1997). Therefore, the distribution of CDOM in open ocean can be regulated by a balance between photobleaching, photohumification, and biogeneration (Ortega-Retuerta et al., 2010a).

Satellite images from the Sea-viewing Wide Field-of-view Sensor (SeaWiFS) have shown that due to the low degree of solar irradiation, deep mixing layer, and high primary productivity, the CDOM exhibits a high-value zone in polar open waters (Siegel et al., 2002). The highest CDOM absorbance at 355 nm of 0.51 m⁻¹ in euphotic layer was recorded in ASP of Southern Ocean, where the dominant phytoplankton taxa, *Phaeocystis antarctica*, was confirmed to be the most important contributor for CDOM (Lee et al., 2016). The net accumulation of CDOM at the surface water of ASP was found to be negative, indicating a labile nature of freshly produced CDOM (Chen et al., 2019). This characteristic was also found in Antarctic Peninsula area, with CDOM half live from 2.1 to 5.1d due to photobleaching in the upper layer (Ortega-Retuerta et al., 2010b). Remote sensing investigations in this area have shown that the seasonal variability of CDOM appeared to be controlled by the dynamics of ice (Ortega-Retuerta et al., 2010b).

Antarctic coastal polynyas experience high primary productivity during the austral spring and summer when there is reduced sea ice coverage (Arrigo and van Dijken, 2003). This increased productivity has significant implications for the carbon cycle in the Southern Ocean. Previously studies have estimated that carbon export in ASP could reach up to 900 mgC m⁻²•d⁻¹ (Yager et al., 2016), and the downward flux of particulate organic carbon (POC) determined by short-term deployment of floating traps at 60 m and 150 m was 320 and 32 mgC•m⁻²•d⁻¹, respectively, indicating an efficient export system (Ducklow et al., 2015). However, only a small fraction of the produced POC can reach the deep layer. As suggested by Lee et al. (2017), the POC flux at \sim 400 m corresponded to 1–2.5% of primary productivity in austral summer. The low POC flux and carbon sequestration in the productive ASP might be influenced by bacterial respiration (Ducklow et al., 2015) and off-shelf flush in the upper layer (Lee et al., 2017). Previous work has identified various FDOM components in ASP (Chen et al., 2019); however, the dynamics for each component in water column are still unclear, especially under the influence of unstable and changing environment such as stratification.

In this study, we investigate the geographic and vertical distribution of CDOM and DOC in ASP, Antarctica. To achieve this, we employ the excitation emission matrix coupled with parallel factor analysis (EEM-PARAFAC) technique. Our objective is to gain a deeper understanding of the sources and variations of CDOM, as well as to identify the factors that influence the dynamics of DOC and CDOM in the highly productive ASP during the austral summer. By analyzing the fluorescence signatures of CDOM and conducting a comprehensive examination of its spatial and vertical distribution, we hope to shed light on the origins and behavior of CDOM in this unique Antarctic ecosystem. Through our research, we aim to contribute to the broader understanding of the biogeochemical processes occurring in the ASP and their implications for carbon cycling in polar regions.

2. Methods

2.1. Study area and sample collection

Samples were collected for DOC and CDOM analysis at austral summer in the Amundsen Sea epipelagic layers during a cruise carried out from January 21st to 30th 2020 on the *R/V Xue Long* of Polar Research Institute of China (PRIC) (Table 1, Fig. 1). The sampling area was divided into two regions based on sea ice concentration data during the survey: the Amundsen Sea Polynya (ASP) and the Amundsen Sea Open Water (ASOW). The polynya in the Amundsen Sea had opened earlier than November 2019, as indicated by sea ice information from that period (Fig. S1). Table 1 and Fig. 1 provide additional details about the samples collected.

At all stations pressure, salinity, and temperature were measured and recorded through a SBE 911 plus CTD, equipped with a rosette sampler with 24×10 L Niskin bottles. The Oxygen concentration was measured by Winkler titration (Williams and Jenkinson, 1982). Oxygen saturation was calculated using the measured data and the solubility equations of Garcia and Gordon (1992) and coefficients of Benson and Krauss Jr. (1984). Apparent Oxygen Utilization (AOU) refers to the consumption of oxygen over that period, which was calculated as difference between oxygen saturation and oxygen at a given depth. AOU could be treated as an indicator of microbial heterotrophic metabolism. Mixed layer depth (MLD) was determined as the depth of the maximum buoyancy frequency according to Carvalho et al. (2016). The index of ice-melting water (%MW) was calculated according to the method of Mendes et al. (2018) using the salinity of the surface ($S_{surface}$) and deep (S_{deep} , about 300 m) seawater, as followed by using Eq. (1):

$$\%MW = \left[1 - \left(S_{\text{surface}} - 6\right) / \left(S_{\text{deep}} - 6\right)\right] \times 100. \tag{1}$$

2.2. Sample treatment

The collected samples for DOC and CDOM analysis were filtered by pre-combusted Whatman GF/F filters, and the filtrate were distributed into two pre-combusted 20 mL glass ampoules and preserved at -20 $^{\circ}\text{C}$ for further analysis in the land laboratory.

2.3. DOC analysis

The DOC analysis was conducted using a Shimadzu TOC-L analyzer based on high temperature combustion. The Milli-Q water (blank) samples were subtracted as a baseline, and standard (42–45 μM C for the DOC, Deep Sea Reference from University of Miami) were measured to check the accuracy of the measurements. Analytical errors based on the replicated measurements, which were at least three measurements per sample, were within 5% of the DOC value.

2.4. CDOM analysis

2.4.1. UV-Vis measurements

CDOM absorbance was measured throughout the UV and visible spectral domains (240–800 nm) with a resolution of 1.0 nm, by using a Shimadzu Spectrophotometer UV-2700 and a 5 cm quartz cuvette. The absorbance (A) was converted into Napierian absorption coefficients (a) by using Eq. (2):

$$a_{\lambda} = 2.303 \times \frac{A_{\lambda}}{I} + k \tag{2}$$

where A_{λ} is the absorbance at the wavelength l and L is the optical pathlength expressed in m and k is an offset calculated as the mean absorbance between wavelengths 650 nm and 700 nm (approximately zero) (Green and Green and Blough, 1994). The Napierian absorption coefficient (a_l) was calculated at 254 nm.

Table 1
Location details in the study area. MLD is the Mixed Layer Depth. %MW is the index of ice-melting water.

Study area	Station	Date (UTC)	Longitude (°)	Latitude (°)	Depth (m)	MLD (m)	%MW
ASOW	A3-08	2020/1/21	-119.84	-69.02	3600	24	5.34
	A3-06	2020/1/23	-119.84	-70.51	2820	15	7.05
	A4-09	2020/1/31	-115.00	-68.00	4480	40	3.07
ASP	A11-02	2020/1/26	-115.01	-72.99	666	28	3.39
	A11-00	2020/1/27	-112.10	-73.99	754	37	0.97
	A4-03	2020/1/27	-112.74	-72.70	437	24	3.87
	A9-01	2020/1/29	-117.00	-73.40	336	24	1.11
	A3-01	2020/1/29	-119.81	-73.02	417	21	3.61
	A3-03	2020/1/30	-120.05	-72.36	1755	12	5.16

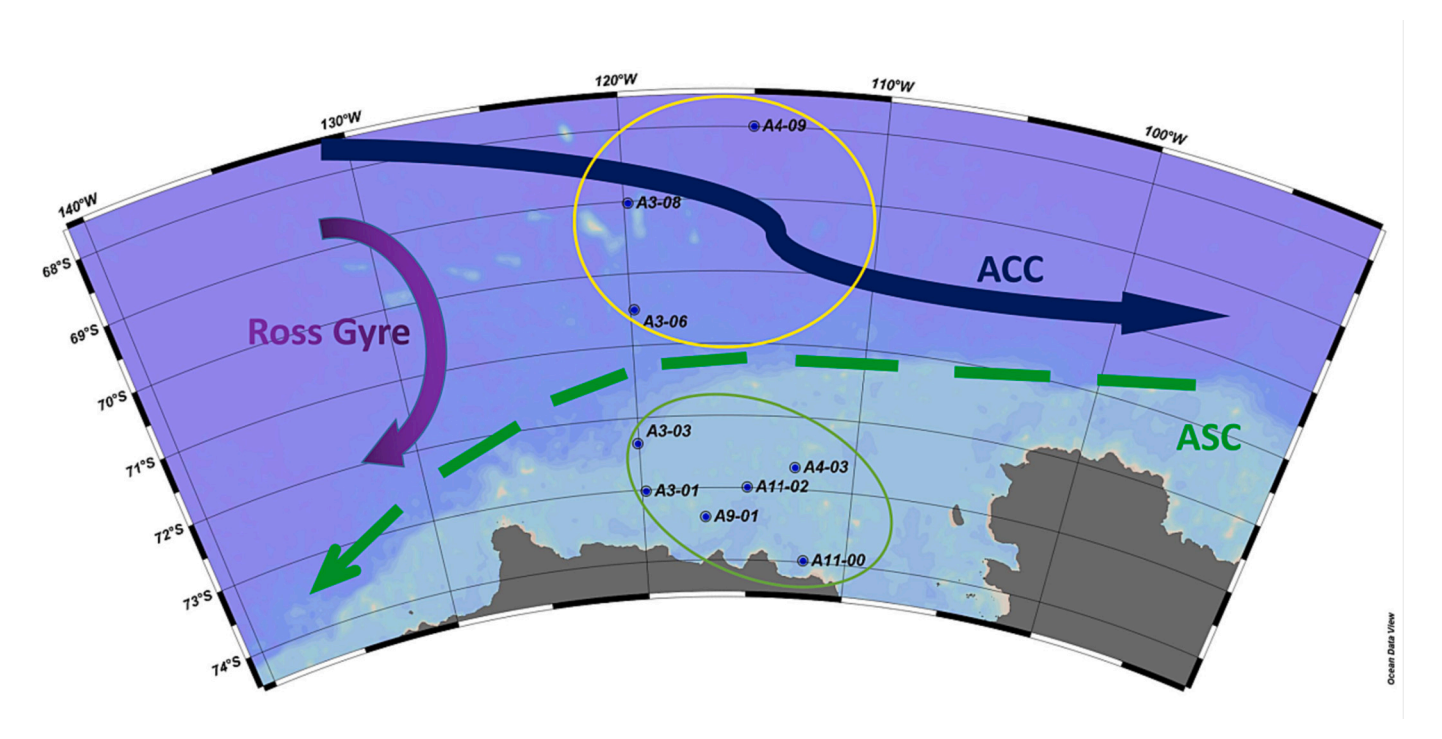


Fig. 1. Location of the stations sampled during austral summer in 2020 cruise. Amundsen Sea Open Water (ASOW) and Amundsen Sea Polynya (ASP) stations were indicated by yellow circles and green circles, respectively. The Antarctic Slope Current (ASC, deep blue), the Antarctic Circumpolar Current (ACC, light green), and Ross Gyre (purple) are also labeled schematically. (For interpretation of the references to colour in this figure legend, the reader is referred to the web version of this article.)

2.4.2. Excitation Emission Matrices (EEMs)

Excitation Emission Matrices (EEMs) were recorded by using the Fluorescence Spectrofluorometer (F4700, Hitachi) with a 1×1 cm quartz cuvette. The excitation range was set from 250 to 450 nm, while the emission range was set from 300 to 600 nm. The excitation and the emission scans were set at 5 nm and 1 nm steps, respectively. Blank subtraction, instrument correction, and Raman Unit normalization were performed. The EEMs were corrected for instrumental bias and subtracted by the EEM of Milli-Q water measured in the same conditions. The Rayleigh and Raman scatter peaks were removed by using the threedimensional interpolation (Zepp et al., 2004). EEMs were normalized to the water Raman signal (Lawaetz and Stedmon, 2009), and the fluorescence intensities were reported as equivalent water Raman Units (R. U.). The EEMs data were further analyzed using the parallel factor analysis (PARAFAC) with the DOMFluor toolbox (Stedmon and Bro, 2008). The four-component model was validated by split-half, random initialization analysis and analysis of residuals. The humification index (HIX) and the biological index (BIX) were calculated from the sample EEMs, as indices for the humification degree and the contribution of biological and autochthonous DOM, respectively (Huguet et al., 2009).

2.5. Analysis of Chl a concentration

For pigment samples, 3 L of seawater was filtered using GF/F glass fiber filter (Whatman, New Castle, U.S.A.) under gentle vacuum (< 0.5 atm) and dim light conditions, and then stored at -80 °C until lab analysis. Prior to instrumental analysis, samples were pre-treated according to the method described in Zapata et al. (2004). The pigments were extracted with 3 mL of acetone, ultrasonicated in an ice bath for 30 s, and then stored at $-20\,^{\circ}\text{C}$ for 2 h. The extract was separated from filter debris, and the supernatant was dried under gentle N2 stream and redissolved with a 300 μ L mixture of methanol and water (9:1 ν/v). The analysis was completed within four hours. Pigment extracts were analyzed using Acquity H-Class Ultra Performance Liquid Chromatography (UPLC, Waters Corp., Milford, U.S.A.) comprising UPLC-Quaternary Solvent Manager, Sample Manager-FTN, PDAe\(\lambda\) Detector, and FLR Detector. The analysis used the Acquity UPLC BEH C18 Column $(50 \times 2.1 \text{ mm}, 1.7 \mu\text{m})$ at a flow rate of 0.4 mL•min⁻¹. A binary gradient elution program was used according to Zapata et al. (2000). Pigments were qualitatively and quantitatively detected by comparing retention time, absorption spectra, and area of the peaks in each sample chromatogram with those of authentic standards purchased from DHI Water and Environment (Hørsholm, Denmark). The detection limits of the

method were 2.20 μ g \bullet L $^{-1}$.

2.6. Statistics

Data plot and statistical analysis were performed with Ocean Data View software (Schlitzer, 2019) and Origin 9.65 software. Differences in response between two categories were assessed with a two-sample t-test, using a p-value of 0.05 or 0.01 to determine statistical significance. The correlations were investigated and considered robust when p < 0.0001 for the whole data-set and p < 0.05 for the single areas.

3. Results

3.1. Water mass and hydrographical conditions

The survey conducted in the Amundsen Sea revealed three prominent water masses based on the vertical profiles of temperature and salinity (Fig. 2). These water masses consist of Antarctic Surface Water (AASW), the relatively cold Antarctic Winter Water (WW), and the warm and salty modified Circumpolar Deep Water (mCDW). AASW exhibited a wide range of temperature, primarily due to the solar radiation, particularly in the center of polynya. It is characterized by low salinity (< 34.1) resulting from the melting of sea ice. Long-time exposure to solar-radiation and the influence of ice-melting water contribute to the stratification of AASW, especially in ASP, with an average MLD of 24 \pm

8 m. The cold WW is situated below AASW, commencing at depths ranging from approximately 30 to 50 m, except for stations A11–00 and A11–01, which exhibit the onset of WW at depths of about 60 to 80 m. WW is characterized by temperatures lower than $-1.5\,^{\circ}$ C. The shelf area of the Amundsen Sea is affected by the intrusion of warm mCDW, with its influence extending even to a water column depth of 200 m in ASOW. Previous studies have also reported similar observations, indicating that the intrusion of CDW occurs through glacially scoured troughs in the seafloor (Jacobs et al., 2012).

3.2. Spatial distributions of Chl a, DO, and AOU

A phytoplankton bloom was observed within the surface mixed layer in ASP, while low levels of *Chl a* concentrations were detected in ASOW (Fig. 3a and d). The mean values of *Chl a* are 5.17 $mg \cdot L^{-1}$ in ASP, and 0.21 $mg \cdot L^{-1}$ in ASOW (Table 2), respectively. The *Chl a* concentrations upon water depth (0-200 m) within ASP are significantly higher than those in ASOW. Typically, high *Chl a* concentrations are usually associated with shallow mixed-layer depth and near-shelf regions (Zhang et al., 2022).

The DO concentrations exhibited a similar distribution pattern to that of *Chl a*, indicating a positive correlation with the phytoplankton bloom (Fig. 3b). The mean values of DO are $10.63 \text{ mg} \cdot \text{L}^{-1}$ in ASP, and $9.92 \text{ mg} \cdot \text{L}^{-1}$ in ASOW (Table 2), respectively. The mean values of AOU are $1.18 \text{ mg} \cdot \text{L}^{-1}$ in ASP, and $1.82 \text{ mg} \cdot \text{L}^{-1}$ in ASOW (Table 2),

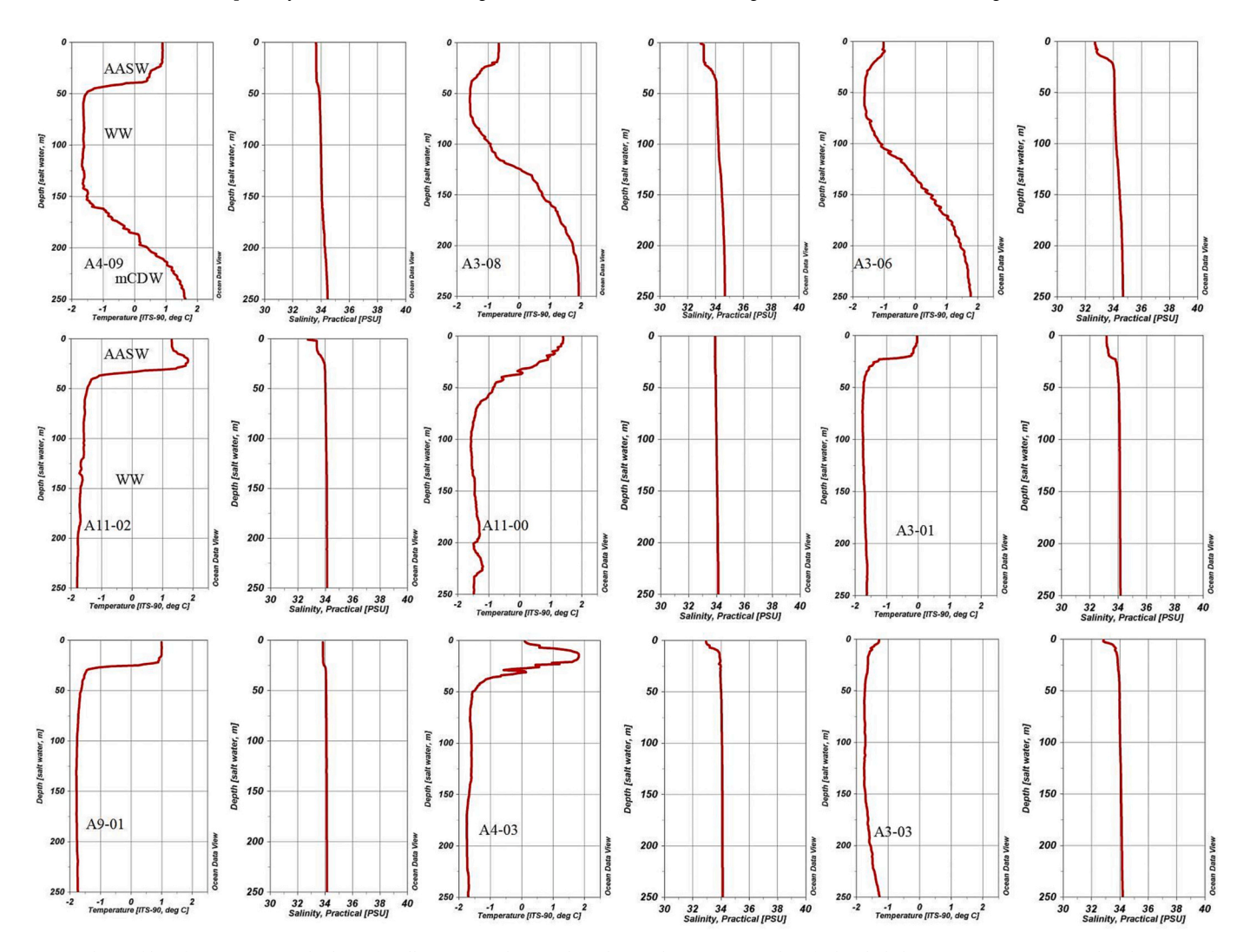


Fig. 2. The profiles of temperature and salinity for all stations in the epipelagic layer. The water mass identified included: Winter Water (WW), modified Circumpolar Deep Water (mCDW), and Antarctic Surface Water (AASW).

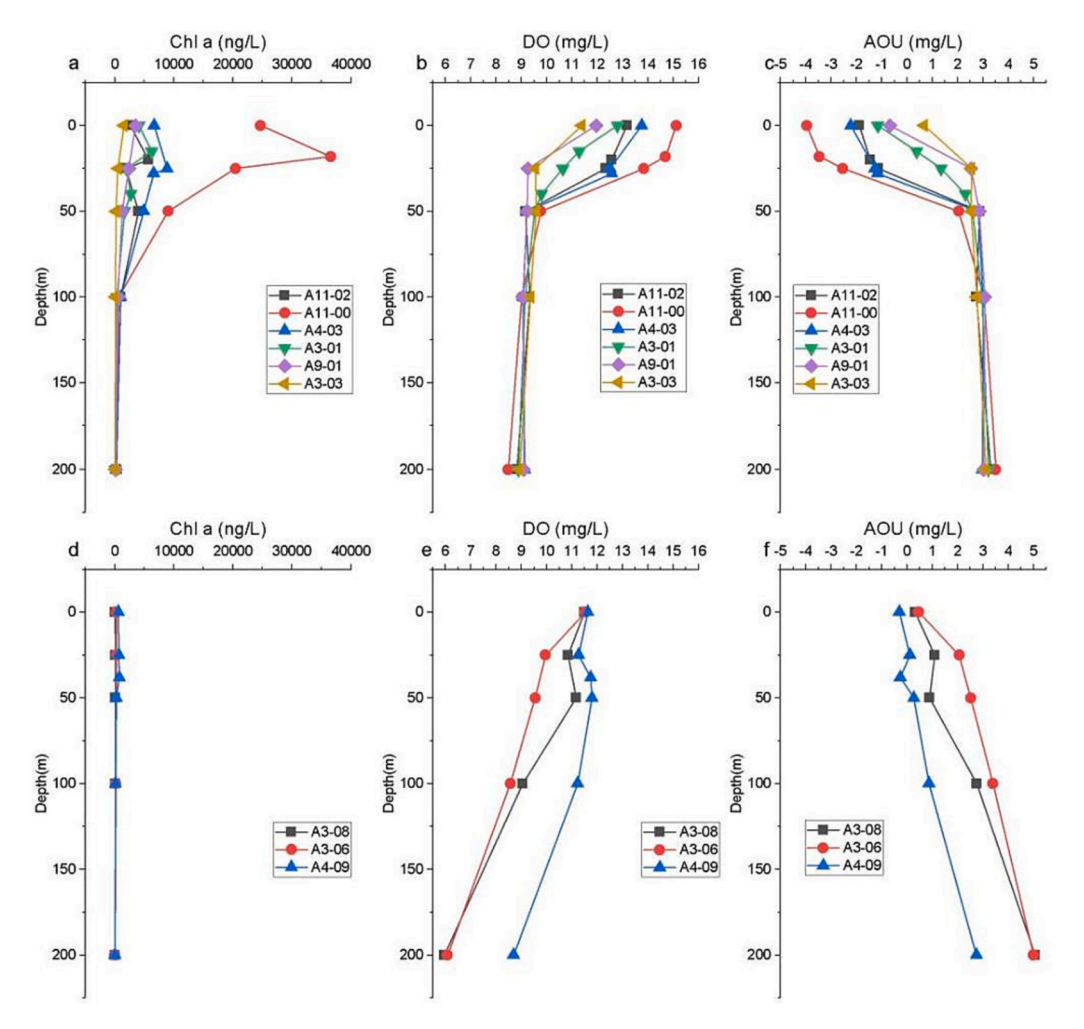


Fig. 3. Profiles of $Chl\ a$ (a and d), DO (b and e), and AOU (c and f) in the Amundsen Sea.

Table 2Mean values and ranges of environmental variables within 200 m in the study area.

Area	$Chl\ a\ (mg \bullet L^{-1})$	DO $(mg \bullet L^{-1})$	DOC $(mg \bullet L^{-1})$	$AOU(mg \bullet L^{-1})$	$a_{254} (m^{-1})$	HIX	BIX
ASOW	0.21	9.92	0.57	1.82	1.01	0.60	1.45
	$ND \sim 0.67$	5.95-11.79	0.46-0.73	-0.31 - 5.06	0.38 - 1.53	0.43-0.88	1.25-1.56
ASP	5.17	10.63	0.49	1.18	2.21	0.59	1.37
	ND ~ 36.58	8.48-15.12	0.35-0.77	-3.96 - 3.51	0.64-6.34	0.43-0.79	1.17-1.53

respectively. High negative values of AOU were observed within the surface mixed layer in ASP, suggesting a strong impact of photosynthesis process. High positive values of AOU were observed at the water depth of 200 m in ASOW, which could be induced by the influence of CDW with warm and salty water. The vertical profiles of AOU displayed sharp gradients around the depths of the mixed layer, which were primarily observed in ASP and not in the open ocean (Fig. 3c and f). This indicates a unique characteristic of the polynya environment.

3.3. HIX, BIX, and PARAFAC components

The mean values of HIX are 0.59 in ASP, and 0.60 in ASOW (Table 2), respectively. The HIX at most stations are <1.00. The mean values of BIX are 1.37 in ASP, and 1.45 in ASOW, respectively. The PARAFAC method was employed in this work, and four fluorophore components were identified using our dataset (Fig. 4a–h and Table 3). Component 1 (C1) has the primary excitation wavelength (Ex) and emission wavelength (Em) of 255 nm and 444 nm, respectively. The second Ex peak with a

lesser intensity was observed at the wavelength of 355 nm. C1 shows spectral characteristics similar to humic-like component (peak A + C) (Coble et al., 1998). Component 2 (C2) and Component 3 (C3) have the Ex/Em of 275 /340 nm and 280 /324 nm, respectively. Both C2 and C3 were identified as protein-like components. C2 shows typical features of tryptophan-like fluorescence. Component 4 (C4) has a primary and secondary excitation peak, occurring around 250 nm or less and 310 nm, respectively, and a single emission peak at 372 nm. This component is characterized by absorption of UVC and UVB light. It is similar to a marine humic-like component (peak M) that occurs at Em 370–420 nm and Ex 290–310 nm (Coble, 1996).

4. Discussion

4.1. In-situ primary productivity as a main source of CDOM in polynya

A phytoplankton bloom was observed in the upper layers of ASP during the survey. The vertical distribution of AOU in ASP suggests that $\,$

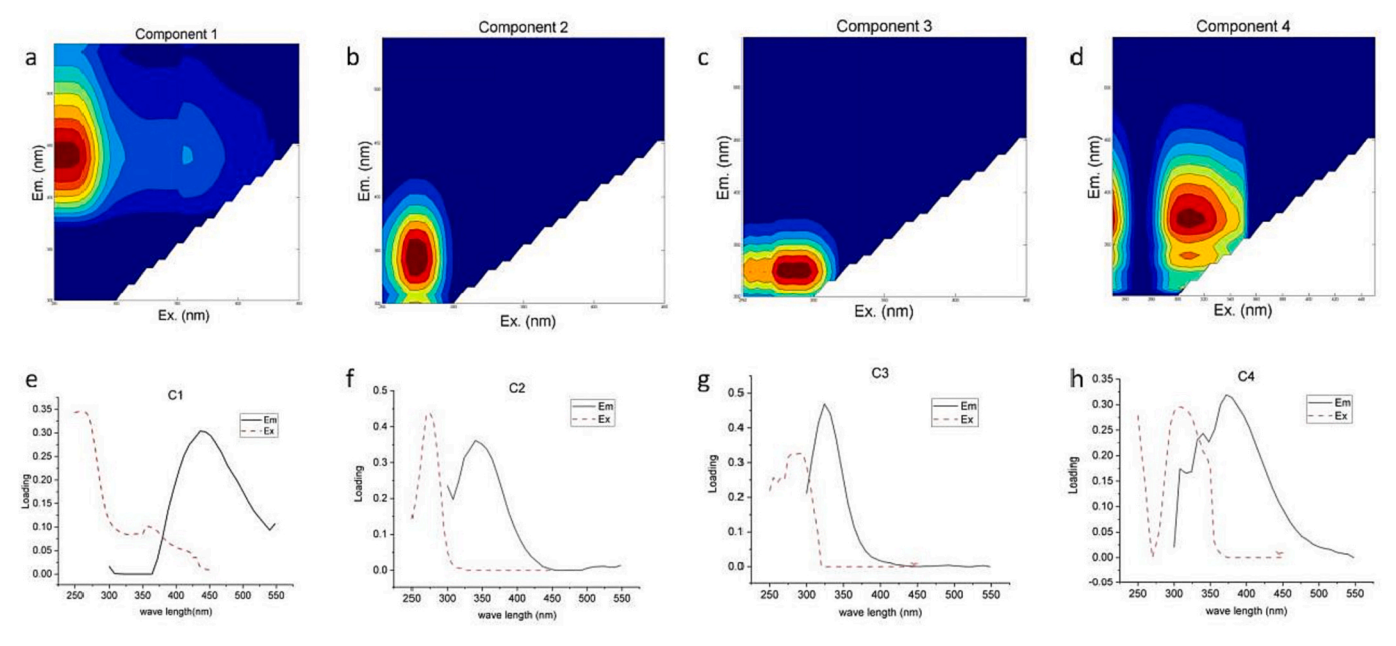


Fig. 4. EEM contour plots of the four different fluorescent components C1–C4 (a - d) identified by PARAFAC, excitation (dash lines) and emission (solid lines) spectra of four components (e–h).

Table 3 Identification of the four PARAFAC components through the comparison with the literature data.

Fluorescent component	Ex/Em	Traditional Identification	Reported literature
C1	255 (355)/ 444	UVC humic-like +UVA humic-like	Coble, 1996; Yamashita and Tanoue, 2003; Stedmon and Markager, 2005; Jørgensen et al., 2011
C2	275/340	protein-like	Coble, 1996; Yamashita and Tanoue, 2003
C3	280/324	protein-like	Burdige et al., 2004; Murphy et al., 2006; Yamashita et al., 2008
C4	(<250) 310/372	UVC humic-like + marine humic-like	Coble, 1996; Zhang et al., 2009; Jørgensen et al., 2011

phytoplankton self-shading had an impact on the euphotic depths, resulting in shallow depths with high Chl concentrations, as previously noted by Oliver et al. (2019). In ASP, bacterial abundance (BA) and bacterial production (BP) exhibited significant correlation with phytoplankton biomass (Hyun et al., 2016). The high abundance of microorganisms, such as phytoplankton and bacteria, indicates a productivity in the upper layer in ASP during our survey. Correlation analyses were conducted on ASP and ASOW, as shown in Table 4. No significant correlations were found between Chl a and DOC or a254 in ASOW. However, in ASP, Chl a concentration showed significant positive correlations with DOC (Spearman correlation coefficient [SCC]: 0.72, p < 0.01) and a_{254} (SCC: 0.74, p < 0.01) in ASP, respectively. Furthermore, the values of the humification index (HIX) (<4) and the bacterial index (BIX) (>1) support the notion that DOM in ASP originates from biological or aquatic bacterial sources, following the findings of Huguet et al. (2009). Previously, Lee et al. (2016) also suggested that CDOM in ASP was significantly associated with chlorophyll, suggesting that Phaeocystis antarctica

Table 4
Comparison of the Spearman correlation coefficient (SCC) in the Amundsen sea.

		AOU	Chl a	DOC	a ₂₅₄	C1	C2	C3	C4	Sanility	HIX
ASOW	Chl a	-0.62*									
	DOC	0.20	-0.21								
	a ₂₅₄	-0.58*	0.29	-0.09							
	C1	0.85**	-0.46	0.46	-0.38						
	C2	0.11	0.38	0.53	0.01	0.36					
	C3	-0.38	0.81**	-0.11	0.02	-0.18	0.55*				
	C4	0.75**	-0.47	0.40	-0.37	0.90**	0.21	-0.05			
	Sanility	0.87**	-0.57*	0.08	-0.37	0.95**	0.21	-0.38	0.83**		
	HIX	0.72**	-0.66**	0.14	-0.22	0.74**	-0.01	-0.59*	0.60*	0.81**	
	BIX	-0.80**	0.59*	-0.35	0.38	-0.88**	-0.09	0.40	-0.86**	-0.78**	-0.85**
ASP	Chl a	-0.67**									
	DOC	-0.46*	0.72**								
	a ₂₅₄	-0.48*	0.74**	0.58**							
	C1	0.19	0.48**	0.38*	0.48**						
	C2	-0.40	0.86**	0.63**	0.60**	0.67**					
	C3	-0.30	0.23	0.22	0.07	0.15	0.29				
	C4	0.15	0.24	0.13	0.22	0.74**	0.42*	-0.01			
	Sanility	0.85**	-0.69**	-0.59**	-0.44**	-0.07	-0.59**	-0.41*	0.14		
	HIX	0.64**	-0.56**	-0.41*	-0.30	0.00	-0.40*	-0.75**	0.08	0.66**	
	BIX	0.01	-0.37*	-0.34	-0.18	-0.57**	-0.47**	0.02	-0.18	0.13	-0.07

^{(**} means p < 0.01; * means p < 0.05)

J. Hu et al. Marine Chemistry 257 (2023) 104329

(*P. antarctica*) played a major role in CDOM production. The disparity observed in the correlation between salinity and DOC in the ASP and ASOW suggests a wide range of sources for DOC in the ASOW. In both ASP and ASOW, salinity exhibits a significant positive correlation with HIX, indicating that the deeper water influenced by the intrusion of mCDW exhibits the characteristic of higher HIX values.

The concentration of *Chl a* shows a positive correlation with major protein-like PARAFAC components C2 (SCC: 0.86, p < 0.01) and huimiclike component C1 (SCC: 0.48, p < 0.01). This suggests that phytoplankton is likely the main source of fluorescent dissolved organic matters (FDOM) in ASP. However, the absence of a positive correlation between Chl a and other protein-like components C3, as well as humiclike component C4, may indicate the presence of additional sources. The emission spectrum of C3 exhibits a blue-shift compared to authentic tryptophan fluorescence. It is known that the fluorescence characteristics of amino acids depends on whether they are freely dissolved or bound in proteins (Lakowicz, 2006). The molecular structure changes such as a decrease in the number of aromatic rings, reduction of conjugated bonds in a chain structure, and conversion of a linear ring system to a non-linear one can result in blue-shift emission of CDOM (Coble, 1996). Therefore, C3 is identified as a blue-shifted tryptophanlike component (Yamashita et al., 2008). Similar components to C3 have been found in coastal ocean of Ise Bay (Yamashita et al., 2008), marine sediment pore waters (Burdige et al., 2004), and ballast water in ship (Murphy et al., 2006). The strong signals of C3 observed at depths around the mixed layer depth (MLD) in ASOW samples A3-06 and A4-09 (Fig. 5c and g), which experience significant influence from icemelting water (evidenced by %MW in sample A3-06 being 7.05%, as

shown in Table 1), along with its occurrence at the surface of ASP, suggest that C3 may serve as a potential tracer for DOC originating from ice-melting water.

The similar C1 component of humic-like substances in the Amundsen Sea waters was also identified by Jeon et al. (2021), characterized by Ex and Em of <250 nm and 448 nm, respectively. However, Chen et al. (2019) identified the tyrosine-like component as C1 using the PARAFAC method based on data from the ASP cruise during the high primary productivity period in the 2016 austral summer. The disparate characteristics of C1 observed in different investigations in ASP may be attributed to variations in CDOM nature resulting from sampling at different bloom stages. In our study, we did not detect strong signals of tyrosine-like fluorescence. Furthermore, in their respective studies, Chen et al. (2019) and Jeon et al. (2021) both identified two similar protein-like components: C_{300/342} and C_{<250(300)/359}, respectively. This kind of component, which might be related to glacier source DOM (Chen et al., 2018), was not detected in our samples. It could probably be explained by the prolonged open period of ASP in our survey and consequently less influenced by melting-water from glacier indicated by %MW information (Table 1). Indeed, the presence of protein-like components related to melting-water from glaciers or seasonal ice has been identified in ASP through previous studies. This suggests a potential relationship between the types of sea ice and the differences observed in Ex and/or Em characteristics of the DOM. Further investigation is necessary to explore this relationship in future studies.

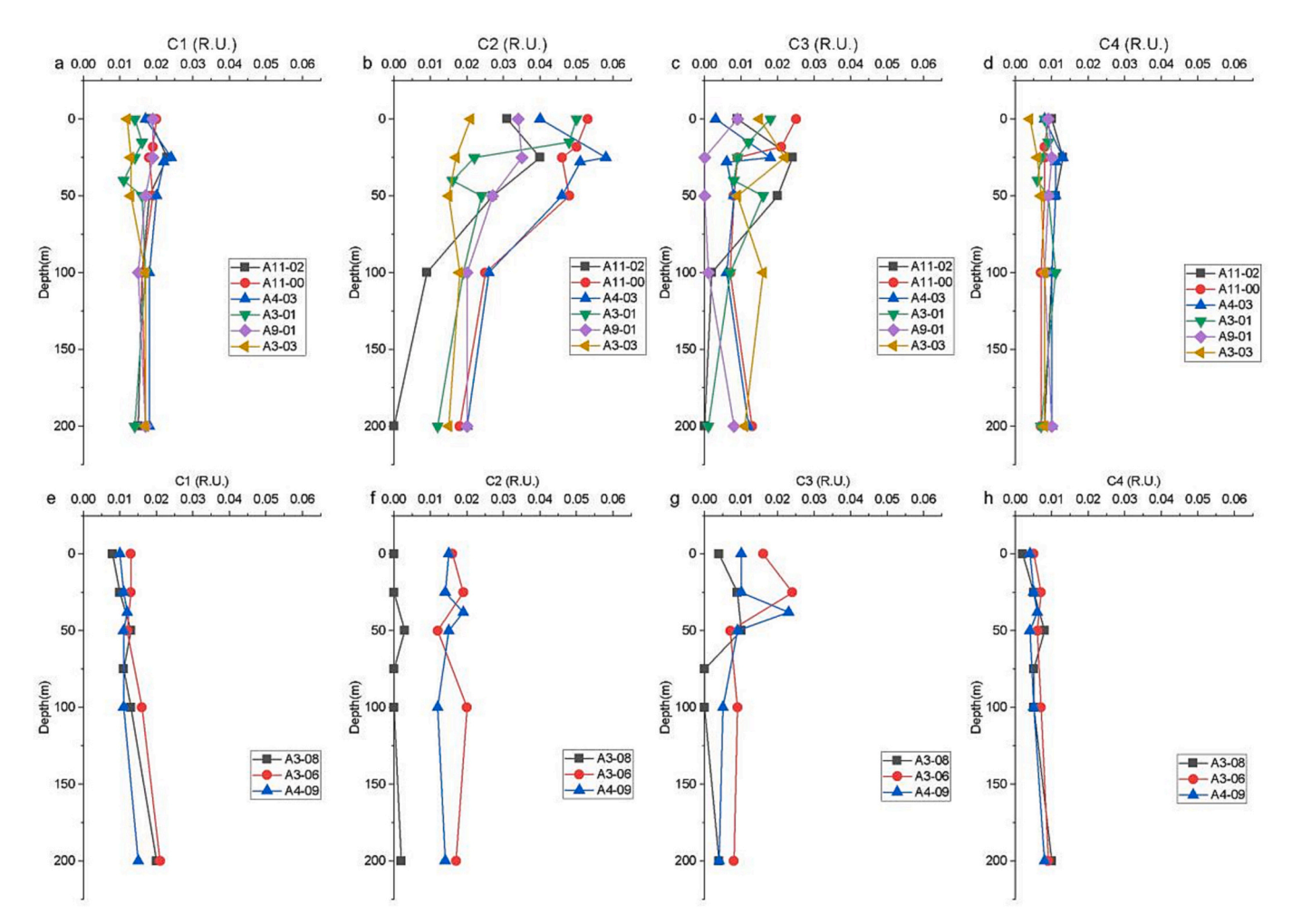


Fig. 5. Depth profile of the EEM components C1(a and e), C2 (b and f), C3 (c and g), and C4 (d and h) in the Amundsen Sea.

4.2. Water mass and biodegradation control the CDOM dynamics upon water depth in polynya

The profiles of DOC and CDOM in ASP indicate the accumulation of these substances within AASW. This accumulation is likely related to the presence of a phytoplankton bloom in the upper layer, as illustrated in Fig. 6. In contrast, the concentration of DOC and relative abundance of CDOM in WW are much lower and exhibit a more uniform distribution. This can be attributed to the mixing processes occurring within the WW. Unlike the AASW, the severe stratification observed in the AASW limits the vertical transport of dissolved and particulate organic matter. As a result, the organic matter remains concentrated within the AASW, leading to higher levels of DOC and CDOM in this region compared to the WW. Furthermore, after conducting a linear regression analysis on

DOC and a254 in ASP (Fig. S2), we observed an Adj. R-Square (R^2) of 0.13. The lower R^2 value can be attributed primarily to the decreased CDOM content in the surface water of three nearshore stations (A11–00, A11–02, and A9–01). This decrease is probably a result of the earlier melting of sea ice in this region, leading to an extended exposure time to solar radiation when surface water temperature exceeds 1 °C. This prolonged exposure causes significant photobleaching, resulting in a substantial reduction of CDOM levels in the surface water. If the effect of photobleaching is not taken into account, the R^2 value would increase to 0.32. A similar effect of photobleaching on CDOM in the surface layer has been previously observed in ASP (Chen et al., 2019).

It has long been recognized that marine phytoplankton is the primary source of CDOM. However, the association between CDOM and phytoplankton is indirect, as bacteria play a crucial role in CDOM production

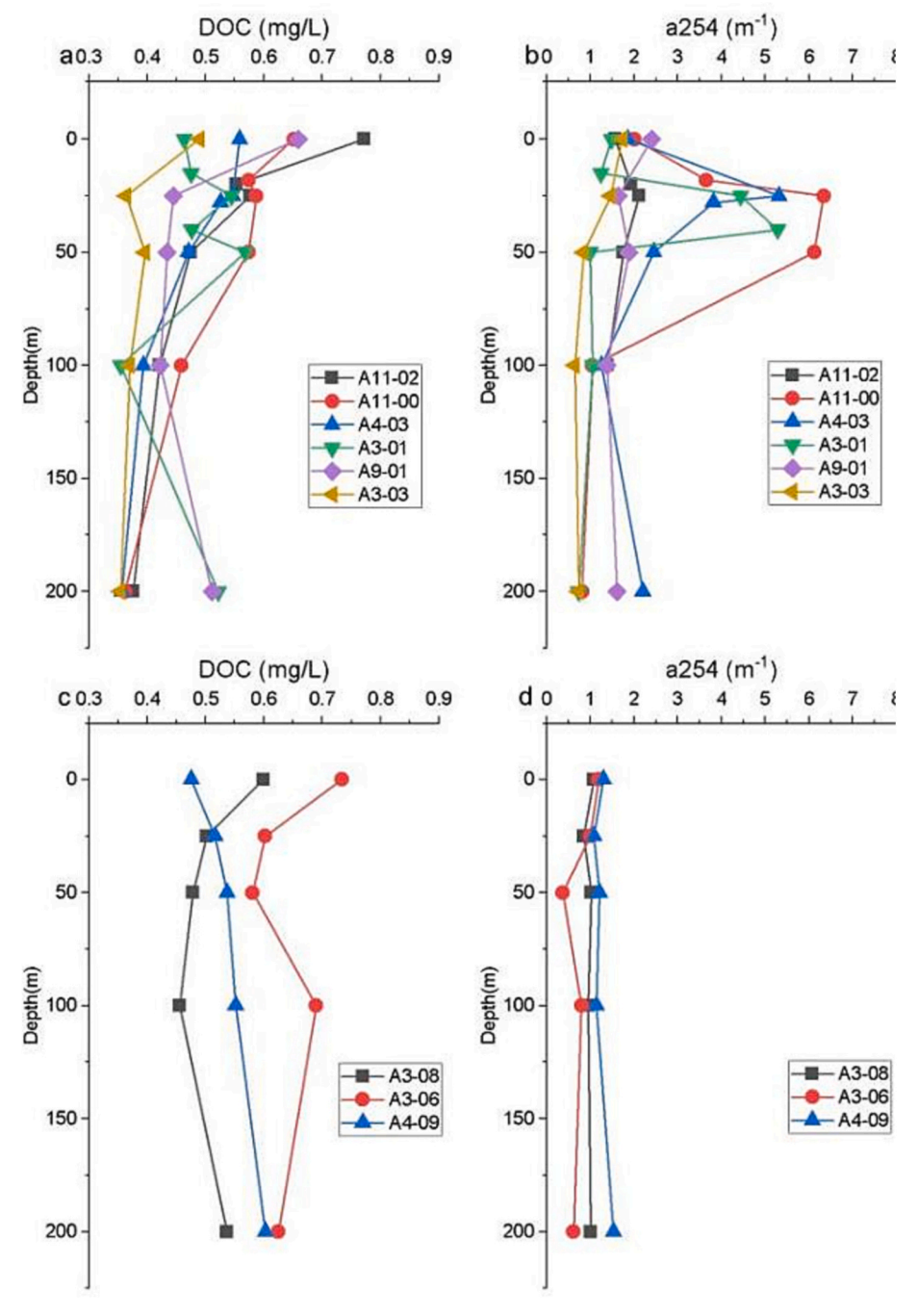


Fig. 6. The vertical distributions of DOC (a and c) and CDOM (b and d) in the Amundsen Sea.

(Cammack et al., 2004; Nelson et al., 1998; Rochelle-Newall and Fisher, 2002). Humic-like component C1 is expected to absorb light in the UVC and UVA regions. The components with similar spectral characteristics were characterized as reduced quinone-like and their spectral loadings were compared to that of the model compound anthrahy- droquinone-2,6-disulfonate (AHDS) (Cory and McKnight, 2005). The long peak excitation and emission wavelengths of C1 indicate that this component consists of large molecular size, hydrophobic compounds (Wu et al., 2003). The similar components have been found in aquatic systems that are dominated by terrestrial and microbial input, and were found in a wide variety of areas such as river (Stedmon et al., 2003), estuary (Stedmon and Markager, 2005), coastal ocean (Coble, 1996), and open ocean (Yamashita and Tanoue, 2003). However, recent research revealed that this type of fluorophores may be intermediate products rather than just a result of terrestrial input (Ishii and Boyer, 2012). The major source of these humic-like components was also considered to be from the microbial turnover of organic matter (Jørgensen et al., 2011). Considering allochthonous and anthropogenic sources of DOM are negligible due to minimum terrestrial input or human impact in the studied area (Dayton et al., 1994), we can take C1 as autochthonous organic matter in water column. C4 component can be attributed to humic-like substances produced in-situ by phytoplankton and microbial activity (Stedmon and Markager, 2005; Murphy et al., 2006; Zhang et al., 2009). This type of fluorophore is similar to those with terrestrial and marine precursors (Ishii and Boyer, 2012). The high levels of C1 and C4 observed in the upper layer of ASP are indicative of elevated microbial activity, which corresponds to the phytoplankton bloom occurring in the euphotic zone. Rochelle-Newall and Fisher (2002) proposed that humic-like fluorescent components are not directly produced by phytoplankton communities, but rather by bacteria through the processing of non-fluorescent organic matter released by phytoplankton. It was widely reported that the production of aquatic humic-like fluorophores is highly correlated with microbial activity (Stedmon and Markager, 2005; Nelson et al., 2010; Yamashita et al., 2010). These humic fluorophores were unlikely to be released directly from cells since their relatively large molecular size (13-150 kDa; Boehme and Wells, 2006), whereas bacterial membranes are permeable to molecules in the size range of 0.5-1 kDa. It was speculated that microbial activity (heterotrophic and autotrophic) in the ocean, including passive release, viral lysis, grazing, and excretion, produces the precursor materials which could extracelluarly form humic materials via abiotic process (Jørgensen et al., 2011).

To investigate the role of microbial heterotrophic respiration in CDOM dynamics, AOU was used as an indicator of microbial heterotrophic metabolism. This analysis excluded AOU values where primary production rates prevailed over respiration rates (i.e., $AOU < 0 \text{ mg} \cdot L^{-1}$) to minimize the effect of primary productivity and exchange with the atmosphere on the AOU distribution. The correlation analysis revealed that AOU is negatively correlated with the DOC (SCC: -0.46, p < 0.05) and CDOM (SCC: -0.48, p < 0.05) in ASP, indicating bacterial decomposition as a main removal pathways of major dissolved organic matters. Additionally, AOU is positively correlated with FDOM components C1 (SCC: 0.85, p < 0.01) and C4 (SCC: 0.75, p < 0.01) in ASOW, confirming the key role of microbial heterotrophic metabolism in the production of humic-like materials in the ocean. Although a positive correlation between AOU and humic-like FDOM components is not observed in ASP due to the mismatch of applied AOU and active heterotrophic metabolism at the same depth, Component C2 provides insight into estimating the extent of bacteria activity at those depths. Trypytophan-like component C2 was widely observed in both open and coastal oceans (Table 3), and its strong fluorescent signal in the shallow waters of ASP potentially suggests the presence of strong bacteria activities (Determann and Lobbes, 1998). The fluorescent signal level of C2 is the highest among the other three components, and its profile shows a strong signal area within 50 m depth of ASP (Fig. 5), potentially suggesting the strong bacteria activities in the shallow water of ASP. The positive correlations

between components C2 and C1 (SCC: 0.67, p < 0.01) and C4 (SCC: 0.42, p < 0.05) provide further evidences for the enhanced bacteria activities (Table 4). Therefore, the physical variables (water mass and solar radiation) and bioprocesses (phytoplankton production and microbial heterotrophic metabolism) may be key factors controlling CDOM dynamic in polynyas.

5. Conclusion

In the 2020 austral summer, we conducted a field survey in a highly productive polynya of Amundsen Sea, and found a phytoplankton bloom in upper water column, with phytoplankton being the main source of DOC and CDOM in ASP. Microbial heterotrophic metabolism was found to be the main pathway of DOC removal and also involved in the dominant production process of humic-like fluorescent components. The CDOM dynamic in polynya was mainly controlled by physical variables (water mass and solar radiation) and bioprocesses (phytoplankton production and microbial heterotrophic metabolism). Lee et al. (2017) suggested that CDW intrudes deep into the Amundsen shelf along the bottom, and the carbon-laden water (fine POC or dissolved carbon forms) flows off the shelf in the upper layer. Our findings also show that average DOC of WW in ASP (0.43 \pm 0.07 mg \bullet L⁻¹, n = 18) is obviously lower than that in ASOW (0.55 \pm 0.08 mg \bullet L⁻¹, n = 6, p < 0.05), indicating a strong conversion of DOC below the surface mixed layer in polynya during the summer bloom at ice-free time. This information could help evaluate whether the export carbon from the surface mixed layer of ASP is flushed off the Amundsen shelf mainly in the form of dissolved inorganic carbon, though further studies on the contribution from glacier-melting water would be needed.

Data availability

The authors do not have permission to share data.

Acknowledgments

The author thanks the Polar Research Institute of China (PRIC) and the crew of R/V Xuelong for their assistance in sample collection and analysis on board. This research was funded by the National Natural Science Foundation of China (No. 42276255 and 41976227), project Impact and Response of Antarctic Seas to Climate Change, IRASCC 2020-2022 (No. 01-01-02A and 02-02-05), and the Scientific Research Fund of the Second Institute of Oceanography, MNR, grand No. JG1715.

Appendix A. Supplementary data

Supplementary data to this article can be found online at $\frac{\text{https:}}{\text{doi.}}$ org/10.1016/j.marchem.2023.104329.

References

Arrigo, K.R., van Dijken, G.L., 2003. Phytoplankton dynamics within 37 Antarctic coastal polynya systems. J. Geophys. Res. 108 (C8), 3271.

Arrigo, K.R., van Dijken, G., Long, M., 2008. Coastal Southern Ocean: a strong anthropogenic CO_2 sink. Geophys. Res. Lett. 35, L21602.

Babin, M., Stramski, D., Ferrari, G.M., Claustre, H., Bricaud, A., Obolensky, G., Hoepffner, N., 2003. Variations in the light absorption coefficients of phytoplankton, nonalgal particles, and dissolved organic matter in coastal waters around Europe. J. Geophys. Res. 108 (C7), 3211.

Benson, B.B., Krauss Jr., D., 1984. The concentration and isotopic fractionation of oxygen dissolved in freshwater and seawater in equilibrium with the atmosphere. Limnol. Oceanogr. 29, 620–632.

Boehme, J., Wells, M., 2006. Fluorescence variability of marine and terrestrial colloids: examining size fractions of chromophoric dissolved organic matter in the Damariscotta River estuary. Mar. Chem. 101, 95–103.

Burdige, D.J., Kline, S.W., Chen, W., 2004. Fluorescent dissolved organic matter in marine sediment pore waters. Mar. Chem. 89, 289–311.

Cammack, W.K.L., Kalff, J., Prairie, Y.T., Smith, E.M., 2004. Fluorescent DOM in lakes: relationships with heterotrophic metabolism. Limnol. Oceanogr. 49, 2034–2045. J. Hu et al. Marine Chemistry 257 (2023) 104329

- Carder, K.L., Steward, R.G., Harvey, G.R., Ortner, P.B., 1989. Marine humic and fulvic acids: their effects on remote sensing of ocean chlorophyll. Limnol. Oceanogr. 34, 60 91
- Carvalho, F., Kohut, J., Oliver, M.J., et al., 2016. Mixing and phytoplankton dynamics in a submarine canyon in the West Antarctic peninsula. J. Geophys. Res.-Oceans 121, 5069–5083.
- Chen, M., Jung, J., Lee, Y.K., et al., 2018. Surface accumulation of low molecular weight dissolved organic matter in surface waters and horizontal off-shelf spreading of nutrients and humic-like fluorescence in the Chukchi Sea of the Arctic Ocean. Sci. Total Environ. 639, 624–632.
- Chen, M., Jung, J., Lee, Y.K., Kim, T.-W., Hur, J., 2019. Production of tyrosine-like fluorescence and labile chromophoric dissolved organic matter (DOM) and low surface accumulation of low molecular weight-dominated DOM in a productive Antarctic Sea. Mar. Chem. 213, 40–48.
- Coble, P.G., 1996. Characterization of marine and terrestrial DOM in seawater using excitation-emission matrix spectroscopy. Mar. Chem. 51, 325–346.
- Coble, P.G., 2007. Marine optical biogeochemistry: the chemistry of ocean color. Chem. Rev. 107, 402–418.
- Coble, P.G., Del Castillo, C.E., Avril, B., 1998. Distribution and optical properties of CDOM in the Arabian Sea during the 1995 southwest monsoon. Deep-Sea Res. Pt II 45, 2195–2223.
- Cory, R.M., McKnight, D.M., 2005. Fluorescence spectroscopy reveals ubiquitous presence of oxidized and reduced quinones in dissolved organic matter. Environ. Sci. Technol. 39, 8142–8149.
- Dayton, P.K., Mordida, B.J., Bacon, F., 1994. Polar marine communities. Am. Zool. 34, 90–99.
- Determann, S., Lobbes, J. örg M., Reuter, R., Rullkötter, J. ürgen, 1998. Ultraviolet fluorescence excitation and emission spectroscopy of marine algae and bacteria. Mar. Chem. 62, 137–156.
- Ducklow, H.W., Wilson, S.E., Post, A.F., Stammerjohn, S.E., Erickson, M., Lee, S., Lowry, K.E., Sherrell, R.M., Yager, P.L., 2015. Particle flux on the continental shelf in the Amundsen Sea polynya and Western Antarctic peninsula. Elementa 3, 000046.
- Garcia, H.E., Gordon, L.I., 1992. Oxygen solubility in seawater: better fitting equations. Limnol. Oceanogr. 37, 1307–1312.
- Green, S.A., Blough, N.V., 1994. Optical absorption and fluorescence properties of chromophoric dissolved organic matter in natural waters. Limnol. Oceanogr. 39, 1903–1916.
- Hansell, D.A., 2002. DOC in the global ocean carbon cycle. In: Hansell, D.A., Carlson, C. A. (Eds.), Biogeochemestry of Marine Dissolved Organic Matter, First ed. Academic Press, San Diego, pp. 685–714.
- Hansell, D.A., Carlson, C.A., 2013. Localized refractory dissolved organic carbon sinks in the deep ocean. Global Biogeochem. Cy. 27, 705–710.
- Huguet, A., Vacher, L., Relexans, S., Saubusse, S., Froidefond, J.M., Parlanti, E., 2009. Properties of fluorescent dissolved organic matter in the Gironde estuary. Org. Geochem. 40, 706–719.
- Hyun, J.H., Kim, S.H., Yang, E.J., et al., 2016. Biomass, production, and control of heterotrophic bacterioplankton during a late phytoplankton bloom in the Amundsen Sea Polynya, Antarctica. Deep-Sea Res. Pt. II 123, 102–112.
- Ishii, S.K.L., Boyer, T.H., 2012. Behavior of reoccurring parafac components in fluorescent dissolved organic matter in natural and engineered systems: a critical review. Environ. Sci. Technol. 46, 2006–2017.
- Jacobs, S., Jenkins, A., Hellmer, H., Giulivi, C., Nitsche, F., Huber, B., Guerrero, R., 2012. The Amundsen Sea and the Antarctic ice sheet. Oceanogr. 25, 154–162.
- The Amundsen Sea and the Antarctic ice sheet. Oceanogr. 25, 154–162. Jeon, M.H., Jung, J., Park, M.O., Aoki, S., Kim, T.W., Kim, S.K., 2021. Tracing circumpolar deep water and glacial meltwater using humic-like fluorescent dissolved organic matter in the Amundsen Sea, Antarctica. Mar. Chem. 235, 104008.
- Jørgensen, L., Stedmon, C.A., Kragh, T., Markager, S., Middelboe, M., Søndergaard, M., 2011. Global trends in the fluorescence characteristics and distribution of marine dissolved organic matter. Mar. Chem. 126, 139–148.
- Kieber, R.J., Seaton, H., 1997. Photooxidation of triglycerides and fatty acids in seawater: implication toward the formation of marine humic substances. Limnol. Oceanogr. 42, 1454–1462.
- Kieber, R.J., Mcdaniel, J., Mopper, K., 1989. Photochemical source of biological substrates in sea water: implications for carbon cycling. Nature 341, 637–639.
- Lakowicz, J.R., 2006. Principles of Fluorescence Spectroscopy. Springer.
- Lawaetz, A.J., Stedmon, C.A., 2009. Fluorescence intensity calibration using the Raman scatter peak of water. Appl. Spectrosc. 63, 936–940.
- Lee, Y.C., Park, M.O., Jung, J., et al., 2016. Taxonomic variability of phytoplankton and relationship with production of CDOM in the polynya of the Amundsen Sea, Antarctica. Deep-Sea Res. Pt. II 123, 30–41.
- Lee, S.H., Hwang, J., Ducklow, H.W., et al., 2017. Evidence of minimal carbon sequestration in the productive Amundsen Sea polynya. Geophys. Res. Lett. 44, 7892–7899.
- Mendes, C.R.B., Tavano, V.M., Kerr, R., et al., 2018. Impact of sea ice on the structure of phytoplankton communities in the northern Antarctic peninsula. Deep-Sea Res. Pt. II 149, 111–123.
- Murphy, K.R., Ruiz, G.M., Dunsmuir, W.T.M., Waite, T.D., 2006. Optimized parameters for fluorescence-based verification of ballast water exchange by ships. Environ. Sci. Technol. 40, 2357–2362.
- Nelson, N.B., Siegel, D.A., 2013. The global distribution and dynamics of chromophoric dissolved organic matter. Annu. Rev. Mar. Sci. 5, 447–476.

Nelson, N.B., Siegel, D.A., Michaels, A.F., 1998. Seasonal dynamics of colored dissolved material in the Sargasso Sea. Deep-Sea Res. Part I 45, 931–957.

- Nelson, N.B., Siegel, D.A., Carlson, C.A., Swan, C.M., 2010. Tracing global biogeochemical cycles and meridional overturning circulation using chromophoric dissolved organic matter. Geophys. Res. Lett. 37, L03610.
- Norman, L., Thomas, D.N., Stedmon, C.A., Granskog, M.A., Papadimitriou, S., Krapp, R. H., et al., 2011. The characteristics of dissolved organic matter (DOM) and chromophoric dissolved organic matter (CDOM) in Antarctic Sea ice. Deep-Sea Res. II 58, 1075–1091.
- Oliver, H., St-Laurent, P., Sherrell, R.M., et al., 2019. Modeling iron and light controls on the summer *Phaeocystis antarctica* bloom in the Amundsen Sea polynya. Global Biogeoche. Cy. 33, 570–596.
- Ortega-Retuerta, E., Frazer, T.K., Duarte, C.M., et al., 2009. Biogeneration of chromophoric dissolved organic matter by bacteria and krill in the Southern Ocean. Limnol. Oceanogr. 54, 1941–1950.
- Ortega-Retuerta, E., Reche, I., Pulido-Villena, E., et al., 2010a. Distribution and photoreactivity of chromophoric dissolved organic matter in the Antarctic Peninsula (Southern Ocean). Mar. Chem. 118, 129–139.
- Ortega-Retuerta, E., Siegel, D.A., Nelson, N.B., et al., 2010b. Observations of chromophoric dissolved and detrital organic matter distribution using remote sensing in the Southern Ocean: validation, dynamics and regulation. J. Mar. Syst. 82, 295–303.
- Osburn, C.L., O'sullivan, D.W., Boyd, T.J., 2009. Increases in the longwave photobleaching of chromophoric dissolved organic matter in coastal waters. Limnol. Oceanogr. 54, 145–159.
- Rochelle-Newall, E.J., Fisher, T.R., 2002. Production of chromophoric dissolved organic matter fluorescence in marine and estuarine environments: an investigation into the role of phytoplankton. Mar. Chem. 77, 7–21.
- Sallee, J.B., Matear, R.J., Rintoul, S.R., Lenton, A., 2012. Localized subduction of anthropogenic carbon dioxide in the Southern Hemisphere oceans. Nat. Geosci. 5, 579–584.
- Schlitzer, R., 2019. Ocean Data View. http://odv.awi.de.
- Schoof, C., 2010. Ice-sheet acceleration driven by melt supply variability. Nature 468, 803–806.
- Siegel, D.A., Maritorena, S., Nelson, N.B., et al., 2002. Global distribution and dynamics of colored dissolved and detrital organic materials. J. Geophys. Res.-Oceans 107, 21-1–21-14.
- Stedmon, C., Bro, R., 2008. Characterizing dissolved organic matter fluorescence with paral- lel factor analysis: a tutorial. Limnol. Oceanogr. Methods 6, 572–579.
- Stedmon, C.A., Markager, S., 2005. Tracing the production and degradation of autochthonous fractions of dissolved organic matter by fluorescence analysis. Limnol. Oceanogr. 50, 1415–1426.
- Stedmon, C.A., Markager, S., Bro, R., 2003. Tracing dissolved organic matter in aquatic environments using a new approach to fluorescence spectroscopy. Mar. Chem. 82, 239–254.
- Williams, P.J.leB, Jenkinson, N.W., 1982. A transportable microprocessor-controlled precise Winkler titration suitable for field station and shipboard use. Limnol. Oceanogr. 27, 576–584.
- Wu, F.C., Evans, R.D., Dillon, P.J., 2003. Separation and characterization of NOM by high-performance liquid chromatography and on-line three-dimensional excitation emission matrix fluorescence detection. Environ. Sci. Technol. 37, 3687–3693.
- Yager, P.L., et al., 2016. A carbon budget for the Amundsen Sea Polynya, Antarctica: estimating net community production and export in a highly productive polar ecosystem. Elementa 4, 1–36.
- Yamashita, Y., Tanoue, E., 2003. Chemical characterization of protein-like fluorophores in DOM in relation to aromatic amino acids. Mar. Chem. 82, 255–271.
- Yamashita, Y., Jaffé, R., Maie, N., Tanoue, E., 2008. Assessing the dynamics of dissolved organic matter (DOM) in coastal environments by excitation emission matrix fluorescence and parallel factor analysis (EEM-PARAFAC). Limnol. Oceanogr. 53, 1900–1908.
- Yamashita, Y., Cory, R.M., Nishioka, J., Kuma, K., Tanoue, E., Jaffé, R., 2010. Fluorescence characteristics of dissolved organic matter in the deep waters of the Okhotsk Sea and the northwestern North Pacific Ocean. Deep-Sea Res. Pt II 57, 1478–1485
- Zapata, M., Rodríguez, F., Garrido, J.L., 2000. Separation of chlorophylls and carotenoids from marine phytoplankton: a new HPLC method using a reversed phase C8 column and pyridine-containing mobile phases. Mar. Ecol. Prog. Ser. 195, 29–45.
- Zapata, M., Jeffrey, S.W., Wright, S.W., et al., 2004. Photosynthetic pigments in 37 species (65 strains) of Haptophyta: implications for oceanography and chemotaxonomy. Mar. Ecol. Prog. Ser. 270, 83–102.
- Zepp, R.G., Sheldon, W.M., Moran, M.A., 2004. Dissolved organic fluorophores in southeastern US coastal waters: correction method for eliminating Rayleigh and Raman scattering peaks in excitation-emission matrices. Mar. Chem. 89, 15–36.
- Zhang, Y., van Dijk, M.A., Liu, M., Zhu, G., Qin, B., 2009. The contribution of phytoplankton degradation to chromophoric dissolved organic matter (CDOM) in eutrophic shallow lakes: field and experimental evidence. Water Res. 43, 4685–4697.
- Zhang, W., Hao, Q., He, J.F., Pan, J.M., 2022. Variability of size-fractionated phytoplankton in the Amundsen Sea during summer. Adv. Polar Sci. 33, 1–13.